iScience

CellPress
OPEN ACCESS

Article

Phagocytosis by stroma confounds coculture studies

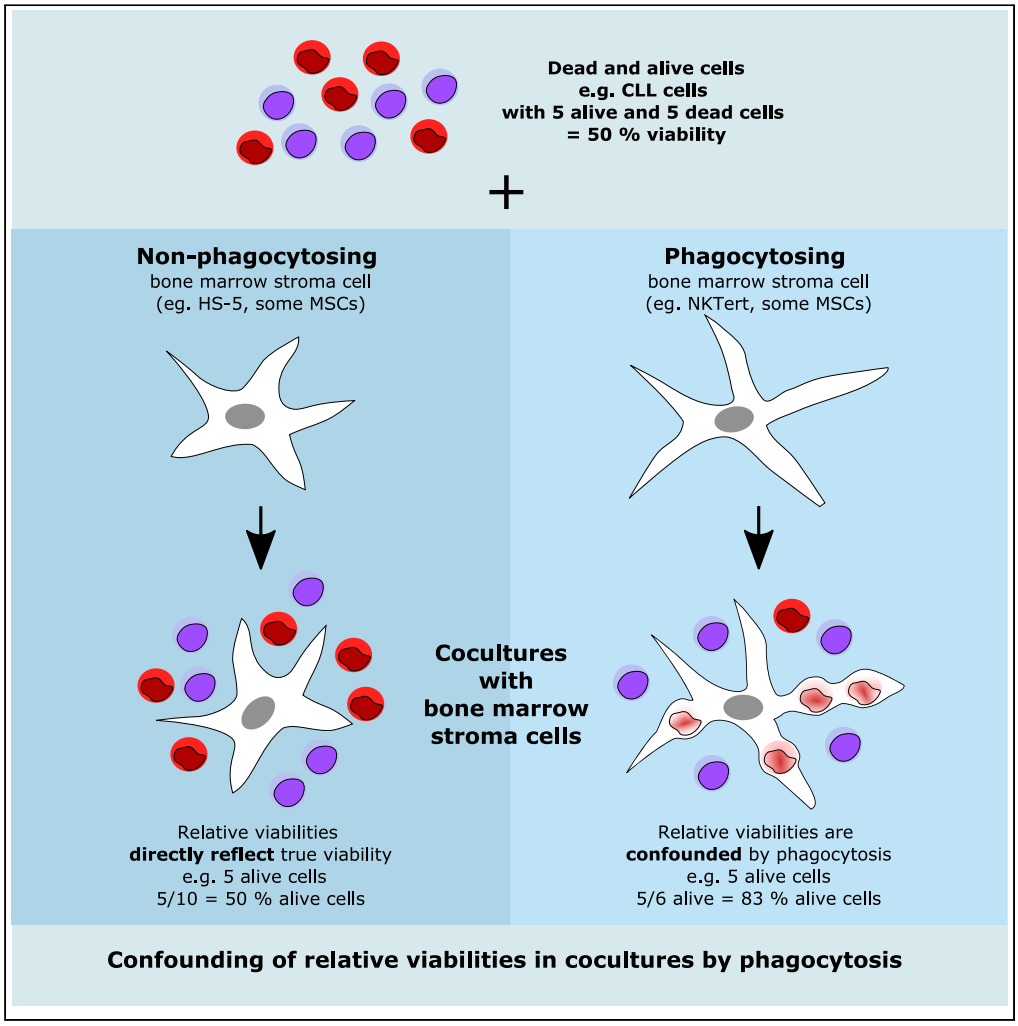

Sophie A. Herbst, Marta Stolarczyk, Tina Becirovic, ..., Marco Herling, Carsten Müller-Tidow, Sascha Dietrich

sascha.dietrich@med.uni-heidelberg.de

Highlights

Some bone marrow stroma cells extensively phagocytose apoptotic cells

Disappearance of dead cells from cocultures due to phagocytosis confounds results

This needs to be considered in studies using relative viabilities in cocultures

Bone marrow stroma cell line NKTert could also phagocytose glass spheres

Herbst et al., iScience 24, 103062
September 24, 2021
https://doi.org/10.1016/j.isci.2021.103062

iScience

CellPress
OPEN ACCESS

Article

Phagocytosis by stroma confounds coculture studies

Sophie A. Herbst,[1,2,3,4,5,8] Marta Stolarczyk,[1,3,8] Tina Becirovic,[1] Felix Czernilofsky,[1,2,3] Yi Liu,[1] Carolin Kolb,[1] Mareike Knoll,[1] Marco Herling,[6,7] Carsten Müller-Tidow,[1,2,3] and Sascha Dietrich[1,2,3,4,9,*]

SUMMARY

Signals provided by the microenvironment can modify and circumvent pathway activities that are therapeutically targeted by drugs. Bone marrow stromal cell coculture models are frequently used to study the influence of the bone marrow niche on *ex vivo* drug response. Here, we show that mesenchymal stromal cells from selected donors and NKTert, a stromal cell line, which is commonly used for coculture studies with primary leukemia cells, extensively phagocytose apoptotic cells. This could lead to misinterpretation of results, especially if viability readouts of the target cells (e.g. leukemic cells) in such coculture models are based on the relative proportions of dead and alive cells. Future coculture studies which aim to investigate the impact of bone marrow stromal cells on drug response should take into account that stromal cells have the capacity to phagocytose apoptotic cells.

INTRODUCTION

Signals provided by the microenvironment protect leukemia cells from spontaneous apoptosis and modify pathway activities which are therapeutically targeted by drugs (Choi et al., 2016; Ten Hacken and Burger, 2016). *In vitro* coculture models of malignant cells and various bone marrow stromal cell types have been frequently used to understand tumor – microenvironment interactions and how these interactions interfere with the response to cancer drugs. Most commonly, cocultures of leukemia cells and the human bone marrow stromal cell lines NKTert and HS-5, or primary mesenchymal stromal cells (MSCs) are used as models of the human bone marrow niche. Several reports suggest that NKTert and other stromal cells protect leukemia cells from spontaneous and drug-induced apoptosis (Balakrishnan et al., 2015; Cheng et al., 2014; Fiorcari et al., 2013; Kurtova et al., 2009; Zhang et al., 2012). Here, we demonstrate that NKTert and primary MSCs from selected donors massively phagocytose apoptotic cells *in vitro*. The clearance of dead cells increases the relative proportion of alive cells in these cocultures, which represents a major source of bias if the viability readout is based on relative proportions of alive and dead cells. In contrast, other cocultures (with some MSCs or HS-5) did not show this behavior, suggesting them as suitable feeder cells for coculture drug response studies.

RESULTS

Dead leukemia cells disappear in cocultures with NKTert

Leukemic cells from four patients with chronic lymphocytic leukemia (CLL) were cultured either alone (monocultures) or in coculture with the NKTert stromal cell line. The monocultures and cocultures were treated with solvent control (DMSO), venetoclax, or fludarabine. After 72 h, the cultures were stained with the nuclear dye SiR-DNA, the viability dye calcein and the dead cell marker propidium iodide (PI). Based on these stainings, we quantified dead and alive CLL cells by flow cytometry and high content confocal microscopy. First, we calculated relative proportions of dead and alive cells. In accordance with the literature (Balakrishnan et al., 2015; Cheng et al., 2014; Fiorcari et al., 2013; Kurtova et al., 2009; Zhang et al., 2012), we could confirm higher proportions of alive CLL cells in cocultures with NKTert stromal cells than in suspension monocultures of CLL cells only. This was true for all untreated and drug treated conditions and could be interpreted as stromal-cell-mediated protection from spontaneous and drug-induced apoptosis (Figure 1A). We further compared absolute CLL cell counts as determined by microscopy and flow cytometry. Surprisingly, we observed much lower absolute CLL cell counts in NKTert cocultures

[1]Department of Medicine V, Hematology, Oncology and Rheumatology, University of Heidelberg, Im Neuenheimer Feld 410, 69120 Heidelberg, Germany

[2]European Molecular Biology Laboratory (EMBL), Heidelberg, Germany

[3]Molecular Medicine Partnership Unit (MMPU), Heidelberg, Germany

[4]Department of Translational Medical Oncology, National Center for Tumor Diseases (NCT) Heidelberg and German Cancer Research Center (DKFZ), Heidelberg, Germany

[5]Faculty of Biosciences, University of Heidelberg, Heidelberg, Germany

[6]Department I of Internal Medicine, Center for Integrated Oncology Aachen-Bonn-Cologne-Duesseldorf (CIO ABCD), University of Cologne, Cologne, Germany

[7]Clinic of Hematology, Cellular Therapy and Hemostaseology, University of Leipzig, Leipzig, Germany

[8]These authors contributed equally

[9]Lead author

*Correspondence: sascha.dietrich@med.uni-heidelberg.de

https://doi.org/10.1016/j.isci.2021.103062

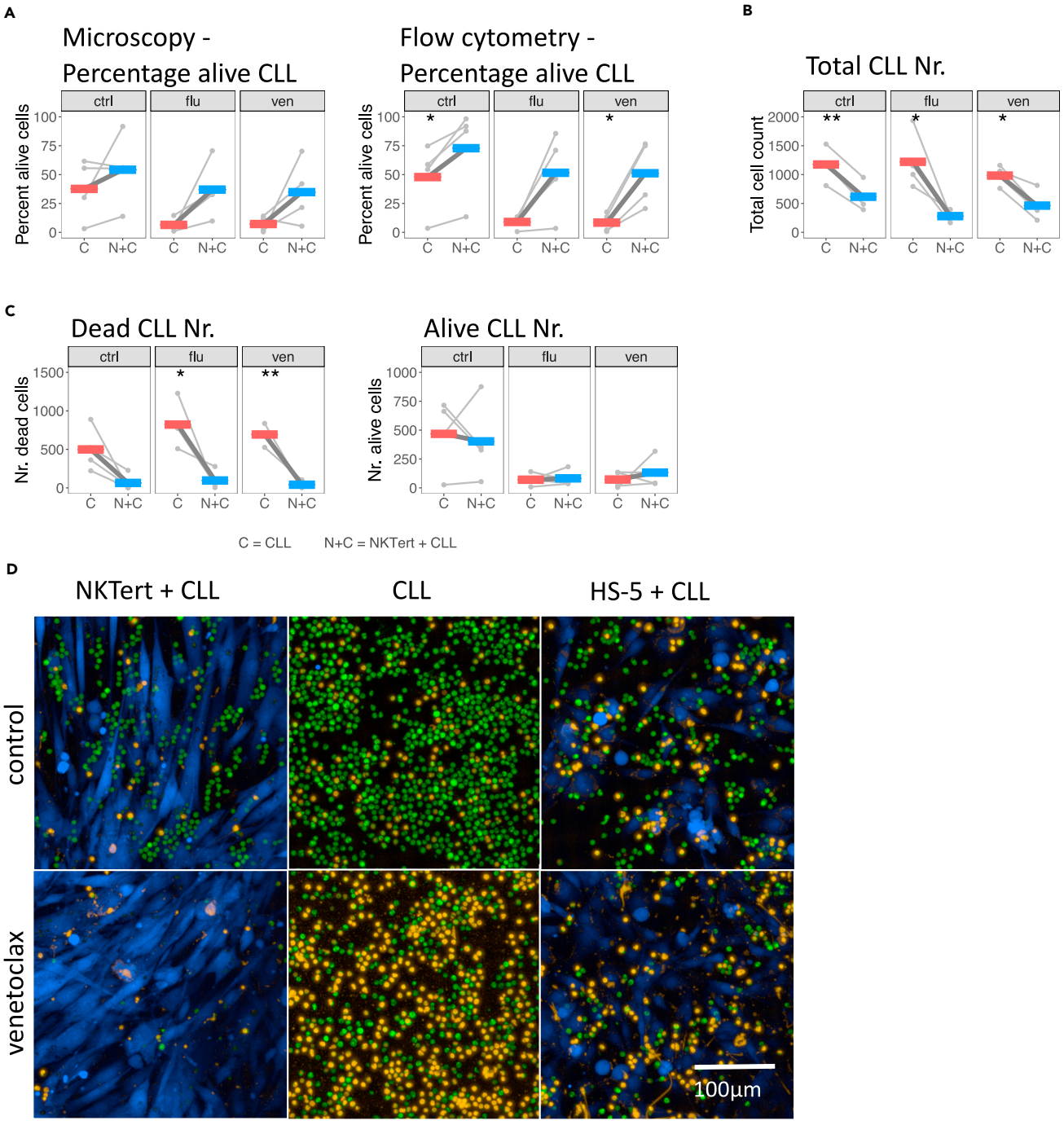

Figure 1. Dead leukemia cells disappear from cocultures of CLL with NKTert bone marrow stromal cells

(A) The percentage of alive CLL cells was higher in cocultures of CLL and NKTert (N + C) than in CLL monocultures (C). This was true for cultures treated with solvent (ctrl), fludarabine (flu) or venetoclax (ven). The readout was either performed with microscopy or flow cytometry; paired t test, * = $p < 0.05$; thin lines = samples from four patients; thick, colored bars = mean.

(B) Total cell counts decreased in solvent control treated (ctrl), fludarabine treated (flu) and venetoclax treated (ven) cocultures of CLL and NKTert (N + C) in comparison to monocultures of CLL (C). Paired t test, ** = $p < 0.01$, * = $p < 0.05$; thin lines = samples from four patients; thick, colored bars = mean, assessed by microscopy.

(C) Dead CLL cells disappeared in cocultures with NKTert. The total number of alive cells was comparable between the culture conditions. Paired t test, ** = $p < 0.01$, * = $p < 0.05$; thin lines = samples from four patients; thick, colored bars = mean, assessed by microscopy.

(D) Confocal microscopy pictures of CLL cells cultured in monocultures or in coculture with NKTert or HS-5 stromal cells. CLL cells disappeared from CLL-NKTert cocultures treated with venetoclax. Green = CellTracker Green, blue = CellTracker Blue, yellow = propidium iodide. See also Figures S1 and S2.

than in CLL monocultures (Figure 1B). This decrease was due to the disappearance of dead cells (Figure 1C, left). Absolute counts of alive cells in the cultures did not differ between monocultures and cocultures with NKTert (Figure 1C, right).

To better understand this finding, we labeled leukemia cells from four other patients with CLL with CellTracker Green, pretreated them with venetoclax and cocultured them with CellTracker Blue labeled NKTert cells (Figure 1D). Apoptotic leukemia cells disappeared after 16 h in coculture with NKTert cells, while apoptotic cells were still present in monocultures. This finding could be confirmed in an additional experiment comprising six more patients with CLL using microscopy (Figure S1) or flow cytometry and annexin/PI staining (Figure S2). We further aimed to understand whether other stromal cells behave in the same way and cocultured venetoclax pretreated CLL cells with the cell line HS-5. Cell counts of CLL cells were comparable between monocultures of CLL cells and cocultures with HS-5 stromal cells. These experiments indicated that apoptotic leukemia cells disappeared in NKTert, but not in HS-5 cocultures, which increased the relative proportion of alive leukemia cells (Figure 1A) and could falsely be interpreted as protection of CLL cells by NKTert from spontaneous or drug-induced apoptosis.

NKTert, but not HS-5, phagocytose dead CLL

Next, we aimed to identify why apoptotic cells disappeared in NKTert cell line cocultures. Especially in the venetoclax-treated cocultures, many CLL cells seemed to be located inside of NKTert, based on bright field microscopy (Figures 2A and S3). Confocal microscopy could confirm the localization of CellTracker-Green-labeled CLL inside of CellTracker-Blue-labeled NKTert (Video S1). Further staining with the lysosomal dye NIR revealed large lysosomal bodies inside NKTert cells (Figure 2B), which had the size and shape of CLL cells. Lysosomal bodies often occurred in regions also positive for CellTracker Green and PI staining and were surrounded by, but did not include, CellTracker Blue staining (Figure 2C and Video S1). Time lapse confocal microscopy revealed that uptake of CellTracker Green-labeled CLL cells by NKTert cells and concurrent formation of these phagosomes inside NKTert cells occurred in less than 10 min (Figure S4). We quantified the amount of phagosomes in three independent experiments (Figure 2D). A high number of phagosomes were present in treated NKTert cocultures, whereas large lysosomal bodies were absent in CLL monocultures, NKTert, or HS-5 stroma monocultures or cocultures of CLL and HS-5 cells. The formation of phagosomes could not be prevented by the addition of the caspase inhibitor zVAD to venetoclax-treated cultures (Figure S5). We concluded that NKTert cells, but not HS-5, phagocytose dying CLL cells and, thereby, clear those cells from the cocultures.

Phagocytosis is not cell-type specific and also some MSCs phagocytose dead cells

We wondered whether phagocytosis by NKTert was specific to CLL cells. To this end, the mantle cell lymphoma cell line HBL-2, the acute myeloid leukemia cell line OCI-AML 2, the carcinoma cell line HELA, and the benign epithelial cell line HEK-293T were exposed to 10 μM doxorubicine, to induce apoptosis. Cells were then cocultured with NKTert cells. NKTert phagocytosed apoptotic cells of all tested cell lines, regardless of their origin (Figures 3A and S6). In conclusion, phagocytic activity by NKTert cells is not limited to CLL cells, but is likely cell type independent.

To further evaluate whether the ability to phagocytose apoptotic cells is restricted to the cell line NKTert or whether it also occurs in primary MSCs, which are a more physiological model of the bone marrow niche than cell lines, we cultured venetoclax treated and CellTracker-Green-labeled primary CLL cells with CellTracker-Blue-labeled primary MSCs from four different healthy donors. Phagocytosed CLL cells were observed in MSCs from two out of four donors (Figure S7). Phagocytosis was especially high in MSC1 culture (Figure 3B, Video S2), while MSC2 only exhibited a low amount of phagocytosis (Figure S7). This shows that not only NKTert but also some but not all primary MSCs are able to phagocytose apoptotic cells.

Further analyses of phagocytic potential of bone marrow stroma cells

Due to the massive phagocytic activity exhibited by NKTert, we assessed whether or not the cells are of macrophagic origin. By performing staining against CD45 followed by flow cytometry, we could show that NKTert are negative for this pan-hematopoietic cell marker and, based on this, are not of monocytic lineage or conventional macrophage differentiation (Figure S8). This confirmed the findings by Kawano et al. (2003). Therefore, the extensive phagocytosis by NKTert cells cannot be explained by a macrophagic origin of these cells.

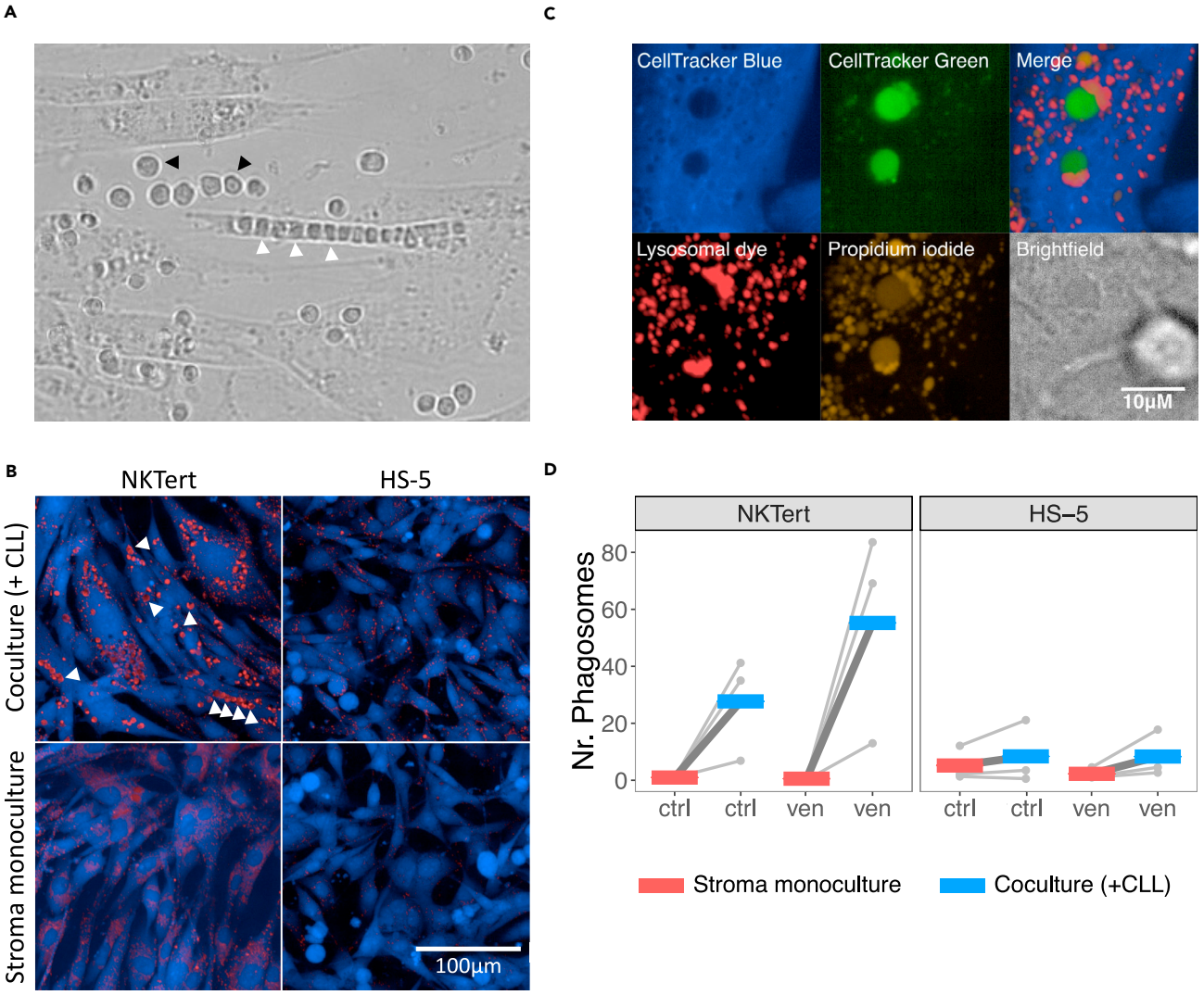

Figure 2. Disappearance of dead leukemia cells is due to extensive phagocytosis by NKTert bone marrow stromal cells

(A) Brightfield image of venetoclax treated NKTert and CLL coculture showing a NKTert cell having phagocytosed many CLL cells. Three of the many phagocytosed CLL cells are highlighted with white arrows, two nonphagocytosed CLL cells are highlighted with black arrows.

(B) Large lysosomal bodies (phagosomes) appeared in cocultures of NKTert and CLL treated with venetoclax. Some of the phagosomes are highlighted with white arrows. Blue = CellTracker Blue, red = lysosomal dye NIR.

(C) Magnification of two phagosomes inside NKTert (CellTracker Blue) cells. CLL cells had been previously labeled with CellTracker Green.

(D) Quantification of phagosomes in microscopy pictures of HS-5 or NKTert stromal monocultures or cocultures with CLL cells. ctrl = solvent control, ven = venetoclax; Points and lines = individual patients, colored bars = mean; samples from three CLL patients. See also Figures S3, S4 and S5.

To further characterize NKTert and HS-5 cells, we performed additional flow cytometry staining with a panel of nine markers and a viability dye (Figure 4A). As expected, HS-5 and NKTert were positive for common MSC markers CD44, CD73, CD90, CD271, CD26, podoplanin, CD31, and CD105 but negative for the endothelial and pericyte marker CD146, thus confirming a mesenchymal origin of NKTert and HS-5 (Li et al., 2016; Lv et al., 2014). Interestingly, NKTert cells displayed a bimodal expression pattern of some markers, including CD90, podoplanin, and CD26, suggesting phenotypic and functional heterogeneity of NKTert. CD90, CD26, and podoplanin have been shown to facilitate fibroblast activation, migration, and extracellular matrix remodeling (Ghersi et al., 2002; Lee et al., 2020; Martín-Villar et al., 2010; Rege et al., 2006; Suchanski et al., 2017).

Since only one out of the two tested human bone marrow stromal cell lines and two out of the four tested MSCs phagocytosed apoptotic cells, we were interested in molecular differences associated with this

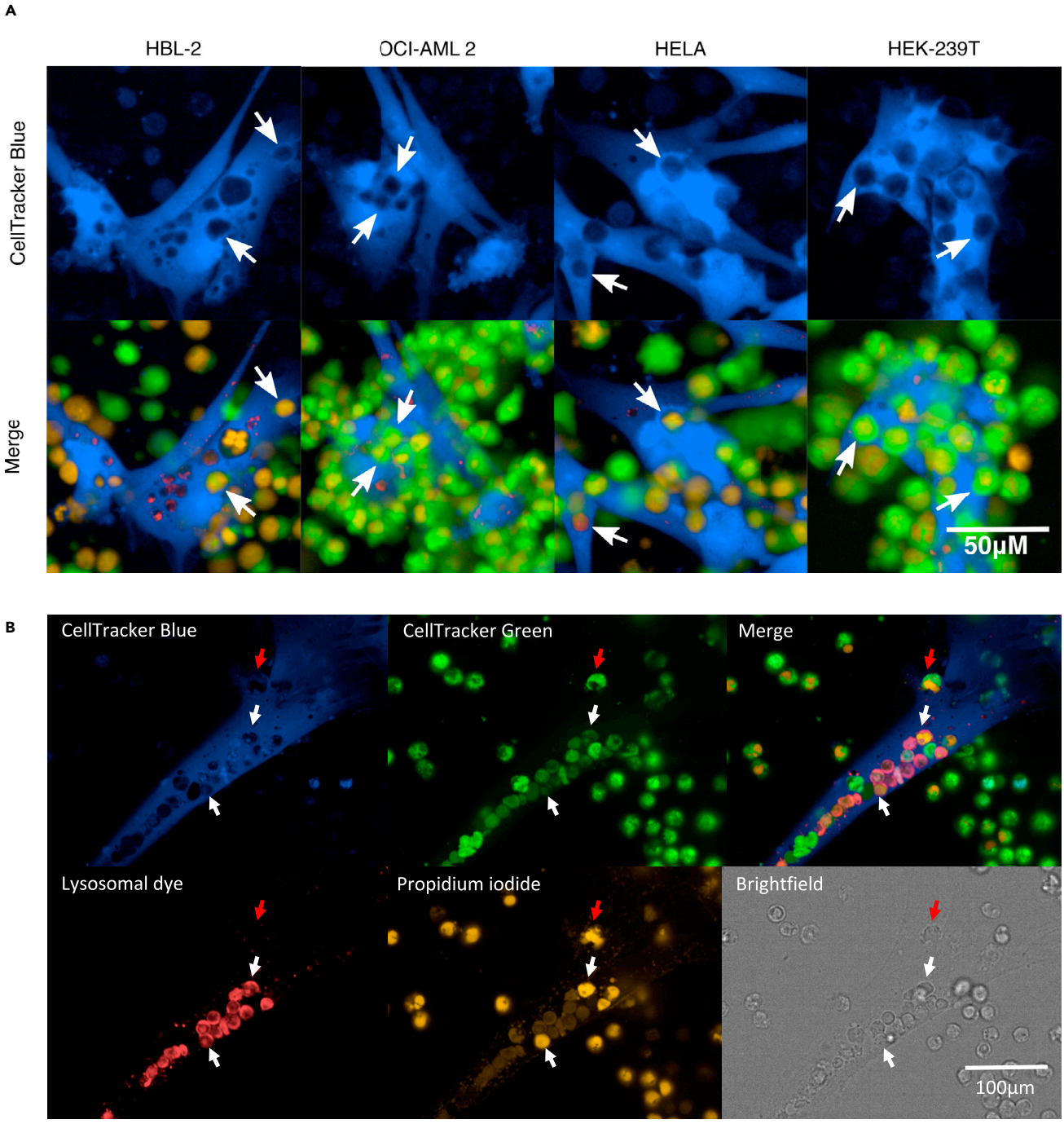

Figure 3. Phagocytosis is not restricted to NKTert but is also observed for MSCs and is not limited to dead cells of leukemic origin

(A) NKTert also phagocytosed apoptotic cells of nonhaematopoietic origin. CellTracker-Green-labeled HBL-2, OCI-AML 2, HELA, or HEK-293T cells (green), treated with doxorubicine to induce apoptosis and cocultured with NKTert. Blank areas in staining of CellTracker-Blue-labeled NKTert (blue) were observed (examples indicated by arrows). These blank areas overlapped with CellTracker-Green (green)- and propidium-iodide (yellow)-stained HBL-2, OCI-AML 2, HELA, or HEK-293T cells. Some of these phagosomes were acidic, indicated by staining with lysosomal dye NIR (red).

(B) CellTracker-Blue-labeled mesenchymal stromal cell (MSC; blue) phagocytosing dead CellTracker-Green-labeled CLL cells (green). White arrows indicate examples for phagosomes containing dead CLL cells. Red arrow indicates dead CLL cell in the process of being phagocytosed by NKTert. See also Video S2 for 3D view. See also Figures S6, S7, Videos S1, and S2.

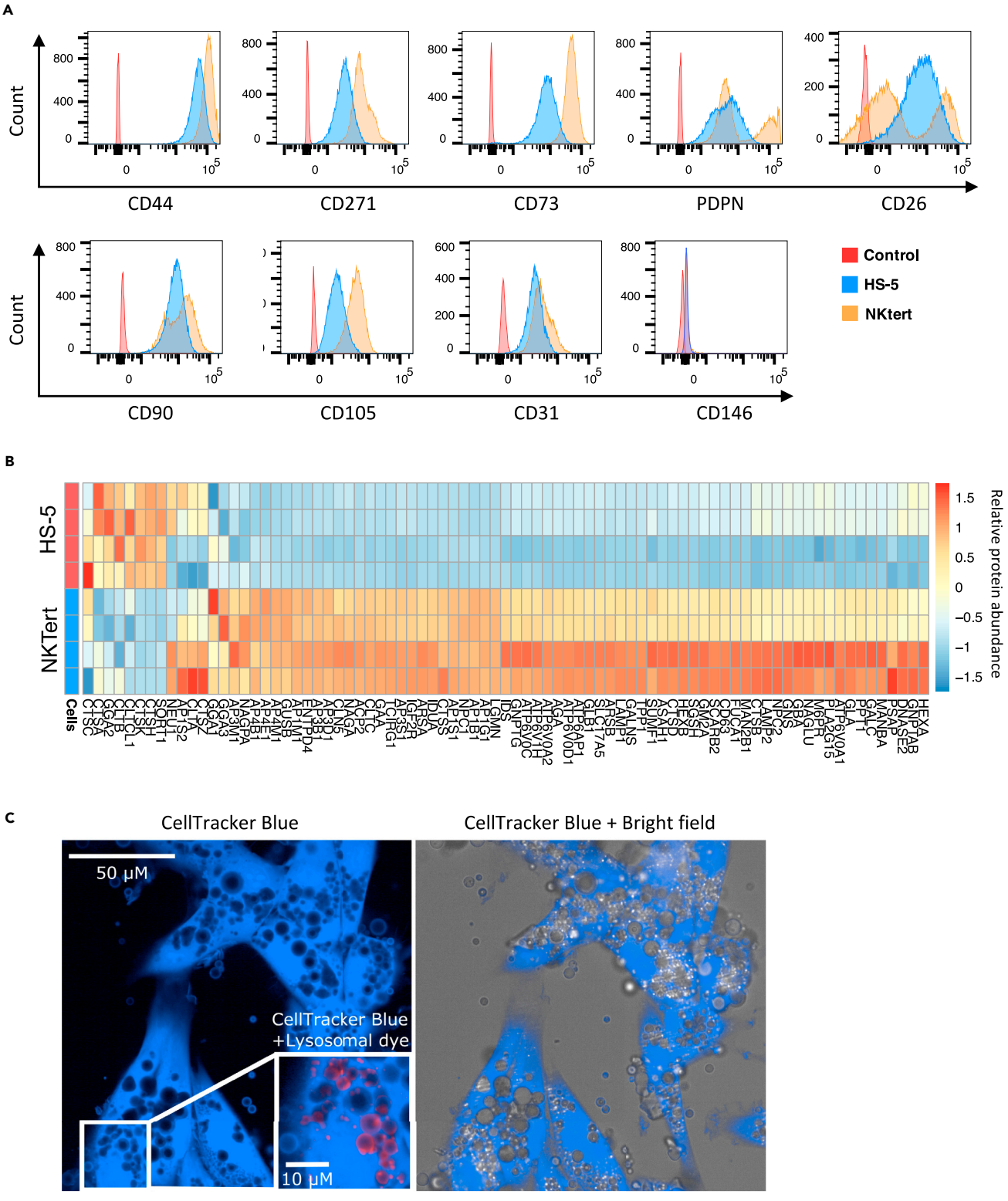

Figure 4. Further characterization of phagocytic potential of bone marrow stromal cell lines

(A) Flow cytometry of HS-5 and NKTert cells stained with antibodies against CD44, CD271, CD73, podoplanin (PDPN), CD26, CD90, CD105, CD31, and CD146.

Figure 4. *Continued*
(B) Relative abundances of proteins in the lysosomal pathway for HS-5 and NKTert stromal cells, assessed by proteomics in four replicates.
(C) Confocal microscopy of CellTracker Blue stained NKTert cocultured with 9- to 13-μM glass spheres for 16 h and stained with lysosomal dye NIR. See also Figures S8, S9, and Data S1.

phagocytic activity. We performed quantitative proteomics of HS-5 and NKTert cells (Data S1). Pathway enrichment analysis on protein abundances revealed that proteins involved in focal adhesion and interaction with the extracellular matrix were significantly upregulated in NKTert cells, which is in accordance with the high abundance of CD90, CD26, and podoplanin in a subpopulation of NKTert. Additionally, the lysosomal pathway was most significantly enriched within differential proteins. Most proteins in this pathway were upregulated in NKTert in comparison to HS-5 (Figure 4B). We observed that blocking the fusion of lysosomes with phagosomes by treatment with chloroquine did not inhibit the uptake of apoptotic cells but prevented acidification of phagosomes and digestion of the content (Figure S9). This could indicate that upregulation of lysosomal proteins may contribute to the phagocytic activity of NKTert, by ensuring the efficient digestion of ingested cells.

Finally, we aimed to assess whether phagocytosis by NKTert cells was mainly triggered by eat-me signals on dead cells or rather prevented by don't-eat-me signals on alive cells. For this we added glass spheres with a particle size of 9–13 μM to CellTracker Blue stained NKTert cultures and assessed the uptake of the spheres after 16 h of culturing. As shown in Figure 4C, NKTert cells ingested large amounts of glass spheres. All analyzed cells had taken up spheres, which indicates that the different populations observed within NKTert in flow cytometry do not possess different phagocytic activities. As described for macrophages (Gilberti et al., 2008), this suggests that the differences between phagocytosis of alive and dead cells by NKTert arise due to the presence of don't-eat-me signals or specific surface charges on the membrane of the target cells.

DISCUSSION

In conclusion, we found that NKTert and selected primary MSCs massively phagocytose apoptotic cells *in-vitro*. Although it has been reported that MSCs are capable of phagocytosis (Dogusan et al., 2004), the extent and consequences for *in vitro* assays have not been anticipated. Phagocytosis leads to the removal of dead cells from the cocultures causing an increased percentage of alive cells, which might be falsely interpreted as a protective effect mediated by stromal cells. This bias might affect flow cytometry assays which rely on the measurement of the relative proportion of alive and dead cells without assessing total cell counts in an *in vitro* culture model. Together this suggests that results from coculture experiments with NKTert or selected MSCs could be misinterpreted if not corrected for this potential bias triggered by the phagocytic activity of these cell types.

There is no doubt that selected bone marrow stromal cells and cell lines are able to protect leukemia cells from spontaneous and drug-induced apoptosis (Lagneaux et al., 1998). For some, but not all stromal cells, this effect might be confounded by their phagocytic activity. The cell line HS-5 for example did not phagocytose apoptotic cells and might therefore be a suitable coculture model system. For future studies, phagocytosis by stromal cells needs to be tested and taken into account, especially as the heterogeneity between cell lines or donors seems to be high. Even though first approaches into this direction have been taken (Baccin et al., 2020; Baryawno et al., 2019), stromal cells are still not sufficiently characterized. Only this will ensure accurate determination of the influence of the microenvironment and, thus, the development of effective treatment strategies.

Limitations of the study

This study demonstrates how phagocytic activity of some bone marrow stromal cells can confound results produced in cocultures with these cells. The presented data do not exclude the fact and do not provide to which extent bone marrow stroma cells possess the ability to protect leukemic cells from apoptosis. This needs to be thoroughly investigated in larger and more comprehensive studies. Additionally, we could show that NKTert cells also phagocytose glass spheres and that, therefore, phagocytosis is most likely dependent on don't-eat-me signals or specific surface charges on the membrane of the target cells. However, the exact mechanism or the factors driving the difference in phagocytic activity between stromal cells remains to be uncovered.

STAR★METHODS

Detailed methods are provided in the online version of this paper and include the following:

- KEY RESOURCES TABLE
- RESOURCE AVAILABILITY
  - Materials availability
  - Lead contact
  - Data and code availability
- EXPERIMENTAL MODEL AND SUBJECT DETAILS
  - Patient samples
  - Cell culture
- METHOD DETAILS
  - Microscopy dyes used in this study
  - Comparing number and percentages of alive and dead cells in mono- and cocultures using microscopy and flow cytometry
  - Visualization of disappearance of leukemia cells and presence of phagosomes by CellTracker and lysosomal staining
  - Validation of disappearance of leukemia cells using Annexin/PI staining and flow cytometry
  - Quantification of the amount of phagosomes
  - Cocultures of NKTert and apoptotic cells of different origins
  - Flow cytometry of CD45
  - Flow cytometry of other markers
  - Cocultures of leukemia cells and primary MSCs using cell tracker
  - Proteomics of HS-5 and NKTert
  - Phagocytosis of glass beads
- QUANTIFICATION AND STATISTICAL ANALYSIS
  - Quantification
  - Statistical analysis

SUPPLEMENTAL INFORMATION

Supplemental information can be found online at https://doi.org/10.1016/j.isci.2021.103062.

ACKNOWLEDGMENTS

SD was supported by a grant of DFG within the SFB 873 and an e:med BMBF junior group grant. CMTs work on MSC was supported by the Deutsche Krebshilfe (70112974) and parts of this work were supported by a grant of the Deutsche Krebshilfe (70172788) to MH. The authors gratefully acknowledge the data storage service SDS@hd supported by the Ministry of Science, Research and the Arts Baden-Württemberg (MWK) and the German Research Foundation (DFG) through grant INST 35/1314-1 FUGG and INST 35/1592-1 FUGG. The authors would like to gratefully acknowledge technical support from the EMBL genomics core facility, the EMBL proteomics core facility and the DKFZ light microscopy facility. We especially thank Per Haberkant, Frank Stein, Vladimir Benes, Nayara Azevedo and Angela Lenze for technical support.

AUTHOR CONTRIBUTIONS

SH, MS, FC, and SD planned the experiments. YL, CK, and MH provided important input for the experimental designs. SH, MS, TB, FC, CK, and MK performed the experiments. SH, MS, and FC analyzed the data. CMT, SD supervised the work. SH, MS, and SD wrote the manuscript. SH and MS contributed equally to this work.

DECLARATION OF INTERESTS

The authors declare no competing interests.

Received: January 14, 2021
Revised: May 20, 2021
Accepted: August 26, 2021
Published: September 24, 2021

REFERENCES

Baccin, C., Al-Sabah, J., Velten, L., Helbling, P.M., Grünschläger, F., Hernández-Malmierca, P., Nombela-Arrieta, C., Steinmetz, L.M., Trumpp, A., and Haas, S. (2020). Combined single-cell and spatial transcriptomics reveal the molecular, cellular and spatial bone marrow niche organization. Nat. Cell Biol. *22*, 38–48.

Balakrishnan, K., Peluso, M., Fu, M., Rosin, N.Y., Burger, J.A., Wierda, W.G., Keating, M.J., Faia, K., O'Brien, S., Kutok, J.L., and Gandhi, V. (2015). The phosphoinositide-3-kinase (PI3K)-delta and gamma inhibitor, IPI-145 (Duvelisib), overcomes signals from the PI3K/AKT/S6 pathway and promotes apoptosis in CLL. Leukemia *29*, 1811–1822.

Baryawno, N., Przybylski, D., Kowalczyk, M.S., Kfoury, Y., Severe, N., Gustafsson, K., Kokkaliaris, K.D., Mercier, F., Tabaka, M., Hofree, M., et al. (2019). A cellular taxonomy of the bone marrow stroma in homeostasis and leukemia. Cell *177*, 1915–1932.e16.

Cheng, S., Ma, J., Guo, A., Lu, P., Leonard, J.P., Coleman, M., Liu, M., Buggy, J.J., Furman, R.R., and Wang, Y.L. (2014). BTK inhibition targets in vivo CLL proliferation through its effects on B-cell receptor signaling activity. Leukemia *28*, 649–657.

Choi, M.Y., Kashyap, M.K., and Kumar, D. (2016). The chronic lymphocytic leukemia microenvironment: beyond the B-cell receptor. Best Pract. Res. Clin. Haematol. *29*, 40–53.

Dogusan, Z., Montecino-Rodriguez, E., and Dorshkind, K. (2004). Macrophages and stromal cells phagocytose apoptotic bone marrow-derived B lineage cells. J. Immunol. *172*, 4717–4723.

Fiorcari, S., Brown, W.S., McIntyre, B.W., Estrov, Z., Maffei, R., O'Brien, S., Sivina, M., Hoellenriegel, J., Wierda, W.G., Keating, M.J., et al. (2013). The PI3-kinase delta inhibitor idelalisib (GS-1101) targets integrin-mediated adhesion of chronic lymphocytic leukemia (CLL) cell to endothelial and marrow stromal cells. PLoS ONE *8*, e83830.

Franken, H., Mathieson, T., Childs, D., Sweetman, G.M., Werner, T., Tögel, I., Doce, C., Gade, S., Bantscheff, M., Drewes, G., et al. (2015). Thermal proteome profiling for unbiased identification of direct and indirect drug targets using multiplexed quantitative mass spectrometry. Nat. Protoc. *10*, 1567–1593.

Ghersi, G., Dong, H., Goldstein, L.A., Yeh, Y., Hakkinen, L., Larjava, H.S., and Chen, W.T. (2002). Regulation of fibroblast migration on collagenous matrix by a cell surface peptidase complex. J. Biol. Chem. *277*, 29231–29241.

Gilberti, R.M., Joshi, G.N., and Knecht, D.A. (2008). The phagocytosis of crystalline silica particles by macrophages. Am. J. Respir. Cell Mol. Biol. *39*, 619–627.

Huber, W., von Heydebreck, A., Sültmann, H., Poustka, A., and Vingron, M. (2002). Variance stabilization applied to microarray data calibration and to the quantification of differential expression. Bioinformatics *18*, S96–S104.

Hughes, C.S., Foehr, S., Garfield, D.A., Furlong, E.E., Steinmetz, L.M., and Krijgsveld, J. (2014). Ultrasensitive proteome analysis using paramagnetic bead technology. Mol. Syst. Biol. *10*, 757.

Kanehisa, M., and Goto, S. (2000). KEGG: kyoto encyclopedia of genes and genomes. Nucl. Acids Res. *28*, 27–30.

Kawano, Y., Kobune, M., Yamaguchi, M., Nakamura, K., Ito, Y., Sasaki, K., Takahashi, S., Nakamura, T., Chiba, H., Sato, T., et al. (2003). Ex vivo expansion of human umbilical cord hematopoietic progenitor cells using a coculture system with human telomerase catalytic subunit (hTERT)-transfected human stromal cells. Blood *101*, 532–540.

Kurtova, A.V., Balakrishnan, K., Chen, R., Ding, W., Schnabl, S., Quiroga, M.P., Sivina, M., Wierda, W.G., Estrov, Z., Keating, M.J., et al. (2009). Diverse marrow stromal cells protect CLL cells from spontaneous and drug-induced apoptosis: development of a reliable and reproducible system to assess stromal cell adhesion-mediated drug resistance. Blood *114*, 4441–4450.

Lagneaux, L., Delforge, A., Bron, D., De Bruyn, C., and Stryckmans, P. (1998). Chronic lymphocytic leukemic B cells but not normal B cells are rescued from apoptosis by contact with normal bone marrow stromal cells. Blood *91*, 2387–2396.

Lee, S.Y., Wu, S.T., Liang, Y.J., Su, M.J., Huang, C.W., Jao, Y.H., and Ku, H.C. (2020). Soluble dipeptidyl peptidase-4 induces fibroblast activation through proteinase-activated receptor-2. Front. Pharmacol. *11*, 552818.

Li, H., Ghazanfari, R., Zacharaki, D., Lim, H.C., and Scheding, S. (2016). Isolation and characterization of primary bone marrow mesenchymal stromal cells. Ann. N. Y. Acad. Sci. *1370*, 109–118.

Lv, F.J., Tuan, R.S., Cheung, K.M., and Leung, V.Y. (2014). Concise review: the surface markers and identity of human mesenchymal stem cells. Stem Cells *32*, 1408–1419.

Martín-Villar, E., Fernández-Muñoz, B., Parsons, M., Yurrita, M.M., Megías, D., Pérez-Gómez, E., Jones, G.E., and Quintanilla, M. (2010). Podoplanin associates with CD44 to promote directional cell migration. Mol. Biol. Cell. *21*, 4387–4399.

Moggridge, S., Sorensen, P.H., Morin, G.B., and Hughes, C.S. (2018). Extending the compatibility of the SP3 paramagnetic bead processing approach for proteomics. J. Proteome Res. *17*, 1730–1740.

Perez-Riverol, Y., Csordas, A., Bai, J., Bernal-Llinares, M., Hewapathirana, S., Kundu, D.J., Inuganti, A., Griss, J., Mayer, G., Eisenacher, M., et al. (2019). The PRIDE database and related tools and resources in 2019: improving support for quantification data. Nucleic Acids Res. *47*, D442–D450.

Rege, T.A., Pallero, M.A., Gomez, C., Grenett, H.E., Murphy-Ullrich, J.E., and Hagood, J.S. (2006). Thy-1, via its GPI anchor, modulates Src family kinase and focal adhesion kinase phosphorylation and subcellular localization, and fibroblast migration, in response to thrombospondin-1/hep I. Exp. Cell Res. *312*, 3752–3767.

Ritchie, M.E., Phipson, B., Wu, D., Hu, Y., Law, C.W., Shi, W., and Smyth, G.K. (2015). Limma powers differential expression analyses for RNA-sequencing and microarray studies. Nucl. Acids Res. *43*, e47.

Savitski, M.M., Wilhelm, M., Hahne, H., Kuster, B., and Bantscheff, M.A. (2015). Scalable approach for protein false discovery rate estimation in large proteomic data sets. Mol. Cell Proteomics *14*, 2394–2404.

Sridharan, S., Kurzawa, N., Werner, T., Günthner, I., Helm, D., Huber, W., Bantscheff, M., and Savitski, M.M. (2019). Proteome-wide solubility and thermal stability profiling reveals distinct regulatory roles for ATP. Nat. Commun. *10*, 1155.

Subramanian, A., Tamayo, P., Mootha, V.K., Mukherjee, S., Ebert, B.L., Gillette, M.A., Paulovich, A., Pomeroy, S.L., Golub, T.R., Lander, E.S., and Mesirov, J.P. (2005). Gene set enrichment analysis: a knowledge-based approach for interpreting genome-wide expression profiles. Proc. Natl. Acad. Sci. U S A *102*, 15545–15550.

Suchanski, J., Tejchman, A., Zacharski, M., Piotrowska, A., Grzegrzolka, J., Chodaczek, G., Nowinska, K., Rys, J., Dziegiel, P., Kieda, C., and Ugorski, M. (2017). Podoplanin increases the migration of human fibroblasts and affects the endothelial cell network formation: A possible role for cancer-associated fibroblasts in breast cancer progression. PLOS One *12*, e0184970.

Ten Hacken, E., and Burger, J.A. (2016). Microenvironment interactions and B-cell receptor signaling in Chronic Lymphocytic Leukemia: implications for disease pathogenesis and treatment. Biochim. Biophys. Acta *1863*, 401–413.

Werner, T., Sweetman, G., Savitski, M.F., Mathieson, T., Bantscheff, M., and Savitski, M.M. (2014). Ion coalescence of neutron encoded TMT 10-plex reporter ions. Anal Chem. *86*, 3594–3601.

Zhang, W., Trachootham, D., Liu, J., Chen, G., Pelicano, H., Garcia-Prieto, C., Lu, W., Burger, J.A., Croce, C.M., Plunkett, W., et al. (2012). Stromal control of cystine metabolism promotes cancer cell survival in chronic lymphocytic leukaemia. Nat. Cell Biol. *14*, 276–286.

STAR★METHODS

KEY RESOURCES TABLE

REAGENT or RESOURCE	SOURCE	IDENTIFIER
Antibodies		
CD146-BV421 (P1H12)	Biolegend	Cat# 361003; RRID: AB_2562966
CD31-BV650 (M89D3)	BD Biosciences	Cat# 744465; RRID: AB_2742254
CD105-FITC (43A3)	Biolegend	Cat# 323203; RRID: AB_755955
CD90-PerCP/Cy5.5 (5E10)	BD Biosciences	Cat# 561557; RRID: AB_10712762
CD44-PE (IM7)	Biolegend	Cat# 103023; RRID: AB_493686
podoplanin-PE/Dazzle (NC-08)	Biolegend	Cat# 337027; RRID: AB_2750287
CD271-PE/Vio770 (ME20.4-1.H4)	Miltenyi Biotec	Cat# 130113984; RRID: AB_2733219
CD26-APC (M-A261)	BD Biosciences	Cat# 563670; RRID: AB_2738363
CD73-APC/Cy7 (AD2)	Biolegend	Cat# 344021; RRID: AB_2566755
Chemicals, peptides, and recombinant proteins		
Hoechst 33342	Invitrogen	Cat# 62249
CellTracker Blue	Invitrogen	Cat# C2111
Calcein	Invitrogen	Cat# C1430
CellTracker Green	Invitrogen	Cat# C7025
SiR-DNA kit	Spirochrome	
Lysosomal Staining Reagent - NIR - Cytopainter	Abcam	Cat# ab176824
Experimental models: Cell lines		
HS-5 cell line	Kind gift by Martina Seiffert, DKFZ	RRID: CVCL_3720
NKTert cell line	RIKEN BRC	RRID: CVCL_4667
Deposited data		
Proteomics data of HS-5 and NKTert	ProteomeXchange Consortium via the PRIDE partner repository	PRIDE: PXD027945
Software and algorithms		
Deposited code	https://github.com/DietrichLab/Phagocytosis	

RESOURCE AVAILABILITY

Materials availability

This study did not generate new unique reagents.

Lead contact

Further information and requests for resources and reagents should be directed to and will be fulfilled by the Lead Contact, Sascha Dietrich (sascha.dietrich@med.uni-heidelberg.de).

Data and code availability

- Microscopy and flow cytometry data reported in this paper will be shared by the lead contact upon request. The mass spectrometry proteomics data have been deposited to the ProteomeXchange Consortium via the PRIDE (Perez-Rivero et al., 2019) partner repository with the dataset identifier PRIDE: PXD027945.
- All original code has been deposited at https://github.com/DietrichLab/Phagocytosis and is publicly available as of the date of publication.

- Any additional information required to reanalyze the data reported in this paper is available from the lead contact upon request.

EXPERIMENTAL MODEL AND SUBJECT DETAILS

Patient samples

In total samples from 18 different CLL patients were used in this study. An overview of the patient samples and for which experiments they have been used can be found in STAR methods table patient overview. Written consent was obtained from patients according to the declaration of Helsinki. The local ethics committee approved the study. Leukemia cells were isolated from blood using Ficoll density gradient centrifugation. Cells were viably frozen and kept on liquid nitrogen until use.

Table patient overview: Overview of patient samples used in this study

Patient	Figure	Gender	IGHV	Trisomy12	TP53/del17p
Patient 1	1	f	U-CLL	Yes	TP53
Patient 2	1	f	U-CLL	No	wt
Patient 3	1	f	U-CLL	No	wt
Patient 4	1	m	M-CLL	No	del17p
Patient 5	2	m	U-CLL	No	wt
Patient 6	2	f	NA	NA	NA
Patient 7	2	m	NA	NA	NA
Patient 8	3a	NA	M-CLL	No	del17p
Patient 9	3b & S6	f	NA	NA	NA
Patient 10	3b & S6	m	M-CLL	No	NA
Patient 11	3b & S6	NA	NA	NA	NA
Patient 12	3b & S6	m	M-CLL	No	wt
Patient 13	S1, S2, S4, S5, S8	f	U-CLL	No	wt
Patient 14	S1, S2, S5, S8	f	U-CLL	No	wt
Patient 15	S1, S2, S5, S8	f	U-CLL	No	TP53
Patient 16	S1, S2, S5, S8	NA	M-CLL	No	wt
Patient 17	S1, S2, S5, S8	m	M-CLL	No	wt
Patient 18	S1, S2, S5, S8	NA	M-CLL	No	TP53&del17p

Cell culture

HS-5 cells were a kind gift by Martina Seiffert. NKTert cells were obtained from RIKEN BRC. Cell lines were maintained in RPMI supplemented with 10% FBS, 1% Penicillin/Streptomycin and 1% Glutamine at 37°C and 5% CO_2 in a humidified atmosphere. Primary MSCs were maintained in MSCGM Mesenchymal Stem Cell Growth Medium Bulletkit medium (Lonza). Cell lines were tested for mycoplasma before all experiments using a PCR based testing procedure. Authentication of HS-5 and NKTert cells was performed (Multiplexion). HS-5 cells could be successfully authenticated. For NKTert no reference sequence was available in the database, however, the NKTert DNA was identified as unique sequence, did not match to any other cell line and, therefore, cross contamination could be excluded.

METHOD DETAILS

Microscopy dyes used in this study

In the study the following dyes for microscopy were used at the indicated concentration. The indicated wave lengths were used for fluorophore excitation: Hoechst 33342 (4 μg/ml, Invitrogen, 405 nm), CellTracker Blue (10 μM, Invitrogen, 405 nm), Calcein (1 μM, Invitrogen, 488 nm), CellTracker Green (10 μM, Invitrogen, 488 nm), propidium iodide (PI; 5 μg/ml, Sigma-Aldrich, 561 nm), SiR-DNA (1 μM, Spirochrome, 640 nm), lysosomal dye NIR (1 μl/ml, Abcam, 640 nm). These dyes were used in the following combinations: Hoechst, Calcein, PI and lysosomal dye NIR, or Calcein, PI and SiR-DNA or CellTracker Blue, CellTracker

Green, PI and lysosomal dye NIR. With the used setup no crosstalk between the channels was seen, with the exception of a slight spillover between calcein and PI and a slight spillover of the signal from the lysosomal dye into the channel for PI.

Comparing number and percentages of alive and dead cells in mono- and cocultures using microscopy and flow cytometry

This section describes the experiment shown in Figures 1A–1C. We cultured cancer cells from four different patients with CLL (2×10^5/well) either alone or in coculture with NKTert (1×10^4/well) in 96-well glass bottom microscopy plates (zell-kontakt GmbH). Stromal cells were seeded 24 hours before the addition of leukemia cells. The samples were treated with solvent control (DMSO), 63 nM venetoclax or 10 μM fludarabine. After 72 hours the cultures were stained with the nuclear dye SiR-DNA, the viability dye Calcein and the dead cell marker PI. Images were taken with the confocal LSM710 microscope (Zeiss) equipped with climate control (37°C, 5% CO_2) using a 20× objective lens. Z-stack images were acquired in triplicate wells, and within one well 4 adjacent fields were imaged.

Directly after acquisition of the confocal microscopy pictures, lymphocytes previously labeled with SiR-DNA, Calcein and PI were pipetted from each cultural condition to a 96-well round bottom plate (Greiner) for further analysis with an IQue Screener (Intellicyt). Calcein and PI signals were recorded. The following gating strategy was pursued: Exclusion of potentially remaining stromal cells, by setting of a lymphocyte gate and exclusion of doublets. The percentage of alive cells was determined by gating on Calcein positive and PI negative cells.

Visualization of disappearance of leukemia cells and presence of phagosomes by CellTracker and lysosomal staining

This section describes the experiment shown in Figures 1D, 1E, S1, S5, and S9. We labeled leukemia cells from four or six other patients with CellTracker Green and cocultured them (2×10^5 cells/well) with CellTracker Blue labeled NKTert (1×10^4 cells/well) or HS-5 (2×10^4 cells/well) stromal cells. CLL cells were pretreated with solvent control or 63 nM venetoclax or 63 nM venetoclax and 10 μM Z-VAD-FMK (Sigma-Aldrich) for 24 hours. For chloroquine treatment, NKTert cells were pretreated with 20 μM hydroxychloroquine for 24 hours. Co-culturing was performed for 16 hours. Cultures were additionally stained with lysosomal dye NIR and PI before imaging. The samples were imaged on an Opera Phenix microscope (Perkin Elmer) in confocal mode. For clearer visualization, the signal from the lysosomal dye is not shown in Figure 1D, while CellTracker Green signal and PI staining are not shown Figure 1E. The images shown are representative of all experiments.

Validation of disappearance of leukemia cells using Annexin/PI staining and flow cytometry

This section describes the experiment shown in Figure S2. We labeled leukemia cells from six patients with CellTracker Green and cocultured them (2×10^5 cells/well) with CellTracker Blue labeled NKTert (1×10^4 cells/well) stromal cells. CLL cells were treated with solvent control or 63 nM venetoclax. After co-culturing for three days samples were harvested by vigorous pipetting. APC Annexin V (RUO; BD Biosciences)/PI staining was performed according to the manufacturer's recommendations. CountBright™ Absolute Counting Beads (ThermoFisher Scientific) were added before measurement. Acquisition was done on a FACSSymphony (BD Biosciences). Compensation, gating on CLL cells, singlets, CellTracker Green positive and CellTracker Blue negative cells was performed before plotting of Annexin against PI intensity. Cell counts were normalized to numbers of counting beads.

Quantification of the amount of phagosomes

This section describes the experiment shown in Figure 1F. The amount of phagosomes was quantified in three independent experiments comprising in total three different CLL patient samples. NKTert cells were seeded at a density of 2.5×10^3 cells/well, HS-5 at a density of 5×10^3 cells/well into wells of a 384 μ-Clear microscopy plate (Greiner) in technical triplicates. After 4 hours CLL cells were added at a density of 5×10^4 cells/well to coculture wells, while additional medium was added to stroma monoculture wells. The cultures were treated with 10 nM Venetoclax or left untreated. After 48 hours the cultures were stained with Hoechst 33342, Calcein, PI and lysosomal dye NIR. Three positions per well were imaged on a CellObserver microscope (Zeiss).

Cocultures of NKTert and apoptotic cells of different origins

This section describes the experiment shown in Figure 2A. To investigate whether phagocytosis by NKTert was specific for dead CLL cells, the mantle cell lymphoma cell line HBL-2, the acute myeloid leukemia cell line OCI-AML 2, the carcinoma cell line HELA or the benign epithelial cell line HEK-293T were detached if adherent and labeled with CellTracker Green. The cells were treated with solvent control or 10 μM doxorubicine to induce apoptosis. This was carried out in 15 mL Falcon tubes to avoid reattachment of the adherent cells. NKTert cells were seeded into wells of a 384 μ-Clear microscopy plate (Greiner) at a density of 2.5×10^3 cells/well and labeled with CellTracker Blue according to the manufacturer's instructions. After incubation for 24 hours, target cells were added to NKTert cells at a density of 2.5×10^4 cells/well. Cocultures of NKTert and CLL cells were used as positive control for the occurrence of phagocytosis. The cultures were stained with PI and lysosomal dye NIR after co-culturing for 16 hours. The samples were imaged on an Opera Phenix microscope (Perkin Elmer) in confocal mode. Representative images are shown.

Flow cytometry of CD45

This section describes the experiment shown in Figure 2B. HEK-293T, HS-5, and NKTert cells were harvested with Accutase (Innovative Cell Technologies) to avoid cleavage of surface epitopes. MCL-2 cells were resuspended. Cells were stained with CD45 (BD Pharmingen™ FITC Mouse Anti-Human CD45, Clone: HI30; BD Biosciences) and analyzed on a LSRII flow cytometer (BD Biosciences).

Flow cytometry of other markers

This section describes the experiment shown in Figure 4A. HS-5 and NKTert cells were harvested with PBS supplemented with 0.02% EDTA to avoid cleavage of surface antigens. Cells were stained with the following antibody conjugates: CD146-BV421 (clone P1H12; Biolegend), CD31-BV650 (M89D3; BD Biosciences), CD105-FITC (43A3; Biolegend), CD90-PerCP/Cy5.5 (5E10; BD Biosciences), CD44-PE (IM7; Biolegend), podoplanin-PE/Dazzle (NC-08; Biolegend), CD271-PE/Cy7 (ME20.4-1.H4; Miltenyi Biotec), CD26-APC (M-A261; BD Biosciences), CD73-APC/Cy7 (AD2; Biolegend) as well as Fixable Viability Dye eFlour 506 (ThermoFisher Scientific). Cells were analyzed on a LSR Fortessa flow cytometer (BD Biosciences). Results are shown as fluorescence intensity histograms gated on live singlets.

Cocultures of leukemia cells and primary MSCs using cell tracker

This section describes the experiment shown in Figure 2C. Primary CLL cells were labeled with CellTracker Green. Apoptosis was induced by treatment with 63 nM venetoclax. After 24 hours the cells (2×10^5 cells/well) were added to primary MSCs of four different healthy donors (1×10^3 cells/well), labeled with CellTracker Blue into 96-well glass bottom microscopy plates (zell-kontakt GmbH). After incubation for 16 hours the cultures were stained with lysosomal dye NIR and PI. The samples were imaged on an Opera Phenix microscope (Perkin Elmer) in confocal mode. Representative images are shown.

Proteomics of HS-5 and NKTert

This section describes the experiment shown in Figure 2D. HS-5 or NKTert cells were trypsinized, washed twice with PBS and snap frozen in liquid nitrogen. HS-5 or NKTert cells were trypsinized, washed twice with PBS and snap frozen in liquid nitrogen. Cell pellets were thawed and resuspended in 50 μl PBS. 50 μl of lysis buffer were added (100 mM Hepes/NaOH pH 8.5, 1% SDS and EDTA-free protease inhibitor). Samples were heated to 95°C for 5 min. DNA and RNA were degraded by the addition of benzonase at 4°C following incubation for 1 h at 37°C. Protein concentrations of lysates were determined by BCA protein determination.

10 μg of each lysate were subjected to an in-solution tryptic digest using a modified version of the Single-Pot Solid-Phase-enhanced Sample Preparation (SP3) protocol (Hughes et al., 2014; Moggridge et al., 2018). To this end, lysates were added to Sera-Mag Beads (Thermo Scientific, #4515-2105-050250, 6515-2105-050250) in 10 μl 15% formic acid and 30 μl of ethanol. Binding of proteins was achieved by shaking for 15 min at room temperature. SDS was removed by 4 subsequent washes with 200 μl of 70% ethanol. Proteins were digested overnight at room temperature with 0.4 μg of sequencing grade modified trypsin (Promega, #V5111) in 40 μl Hepes/NaOH, pH 8.4 in the presence of 1.25 mM TCEP and 5 mM chloroacetamide (Sigma-Aldrich, #C0267). Beads were separated, washed with 10 μl of an aqueous solution of 2% DMSO and the combined eluates were dried down.

Peptides were reconstituted in 10 µl of H2O and reacted for 1 h at room temperature with 80 µg of TMT10plex (Thermo Scientific, #90111) (Werner et al., 2014) label reagent dissolved in 4 µl of acetonitrile. Excess TMT reagent was quenched by the addition of 4 µl of an aqueous 5% hydroxylamine solution (Sigma, 438227). Peptides were reconstituted in 0.1% formic acid, mixed to achieve a 1:1 ratio across all TMT-channels and purified by a reverse phase clean-up step (OASIS HLB 96-well µElution Plate, Waters #186001828BA).

Peptides were subjected to an offline fractionation under high pH conditions (Hughes et al., 2014). The resulting 12 fractions were then analyzed by LC-MS/MS on an Orbitrap Fusion Lumos mass spectrometer (Thermo Scientific) as previously described (Sridharan et al., 2019). To this end, peptides were separated using an Ultimate 3000 nano RSLC system (Dionex) equipped with a trapping cartridge (Precolumn C18 PepMap100, 5 mm, 300 µm i.d., 5 µm, 100 Å) and an analytical column (Acclaim PepMap 100. 75 × 50 cm C18, 3 mm, 100 Å) connected to a nanospray-Flex ion source. The peptides were loaded onto the trap column at 30 µl per min using solvent A (0.1% formic acid) and eluted using a gradient from 2 to 40% Solvent B (0.1% formic acid in acetonitrile) over 2 h at 0.3 µl per min (all solvents were of LC-MS grade). The Orbitrap Fusion Lumos was operated in positive ion mode with a spray voltage of 2.4 kV and capillary temperature of 275°C. Full scan MS spectra with a mass range of 375–1500 m/z were acquired in profile mode using a resolution of 120,000 (maximum fill time of 50 ms or a maximum of 4e5 ions (AGC) and a RF lens setting of 30%. Fragmentation was triggered for 3 s cycle time for peptide like features with charge states of 2–7 on the MS scan (data-dependent acquisition). Precursors were isolated using the quadrupole with a window of 0.7 m/z and fragmented with a normalized collision energy of 38. Fragment mass spectra were acquired in profile mode and a resolution of 30,000 in profile mode. Maximum fill time was set to 64 ms or an AGC target of 1e5 ions). The dynamic exclusion was set to 45 s.

Acquired data were analyzed using IsobarQuant (Franken et al., 2015) and Mascot V2.4 (Matrix Science) using a reverse UniProt FASTA Homo sapiens database (UP000005640 from May 2016) including common contaminants. The following modifications were taken into account: Carbamidomethyl (C, fixed), TMT10plex (K, fixed), Acetyl (N-term, variable), Oxidation (M, variable) and TMT10plex (N-term, variable). The mass error tolerance for full scan MS spectra was set to 10 ppm and for MS/MS spectra to 0.02 Da. A maximum of 2 missed cleavages were allowed. A minimum of 2 unique peptides with a peptide length of at least seven amino acids and a false discovery rate below 0.01 were required on the peptide and protein level (Savitski et al., 2015). Data were processed in the R programming language. The raw output files of IsobarQuant (protein.txt – files) were loaded. For the analysis only proteins quantified with at least two unique peptides were considered, leading to 6657 proteins passing the quality control filters. First, raw signal-sums (signal_sum columns) were cleaned for batch effects using limma (Ritchie et al., 2015). Further normalizations was performed with variance stabilization normalization vsn (Huber et al., 2002). Differentially abundant proteins were analyzed using limma (Ritchie et al., 2015). Information about replicates was added as a factor in the design matrix. Gene set enrichment analysis for the KEGG pathways (Kanehisa and Goto, 2000) was performed using GSEA (Subramanian et al., 2005). A heatmap of the protein abundance of proteins in the lysosomal pathway was visualized using R. Differentially abundant proteins were analyzed using limma (Ritchie et al., 2015). Information about replicates was added as a factor in the design matrix. Gene set enrichment analysis for the KEGG pathways (Kanehisa and Goto, 2000) was performed using GSEA (Subramanian et al., 2005). A heatmap of the protein abundance of proteins in the lysosomal pathway was visualized using R. The mass spectrometry proteomics data have been deposited to the ProteomeXchange Consortium via the PRIDE (Perez-Riverol et al., 2019) partner repository with the dataset identifier PXD027945.

Phagocytosis of glass beads

We tested whether the presence of eat-me signals in general is a requirement for phagocytosis by NKTert. For this, we cultured CellTracker Blue labeled NKTert cells for 24 hours in wells of a 384 Greiner µClear plate, before addition of uncoated glass beads (Sigma Aldrich glass spheres 9- to 13-µm particle size; KatNr.: 440345-100g) washed twice with PBS. After 16 h, the cultures were washed twice with RPMI + 10 % FBS to remove non-phagocytosed beads. After staining with lysosomal dye NIR, the cells were imaged on an Opera Phenix microscope in confocal mode.

QUANTIFICATION AND STATISTICAL ANALYSIS

Quantification

Comparing number and percentages of alive and dead cells in mono- and cocultures using microscopy and flow cytometry. Image analyses were performed on all acquired images using KNIME software. Viability of the lymphocytes was calculated based on the Calcein and PI signals in the z-stack images that correspond to live and dead cells, respectively. After background subtraction using a 'rolling ball' method (radius: 10) and a global threshold was applied (Huang method). Objects were separated using Watershed. Total cell counts were obtained based on SiR-DNA signal (labeling filter: 25-250 pixels). Live/dead cell populations were classified based on the intensity histogram of Calcein and PI signal with a selection of the threshold separately for each cell culture condition: CLL cell culture, and coculture of CLL cells with NKtert cells or HS-5 cells.

Quantification of the amount of phagosomes. The number of phagosomes was quantified in all acquired images using a custom script written in R, with the help of the EBImage package. In brief, a global threshold was applied on the signal from the lysosomal channel, followed by a filling of holes with the fillHull function. To separate objects in close proximity a watershed operation was performed on the distance map of foreground and background pixels. Only objects ranging between 100 and 1500 pixels in size and a circularity of more than 0.8 were classified as phagosomes.

Statistical analysis

Figures 1: Four biological replicates. Paired t-test, ** = $p < 0.01$, * = $p < 0.05$; thin lines = samples from four patients; thick, colored bars = mean.

Figure 2D: Three biological replicates. Points and lines = individual patients, colored bars = mean.

Figure 4B: Differentially abundant proteins were analyzed using limma (Ritchie et al., 2015). Gene set enrichment analysis for the KEGG pathways (Kanehisa and Goto, 2000) was performed using GSEA (Subramanian et al., 2005).

Figures S1 and S2: Six biological replicates. Paired t test, **** = p 0.0001, *** = p 0.001 ** = $p < 0.01$; thin lines = samples from six patients; thick, colored bars = mean.